Graz University of Technology

Total Roto-Translational Variation

Thomas Pock

Institute of Computer Graphics and Vision, Graz University of Technology

Workshop I: Geometric Processing
April 1st, 2019

Joint work with Antonin Chambolle, Ecole Polytechnique Paris

Subjective boundaries

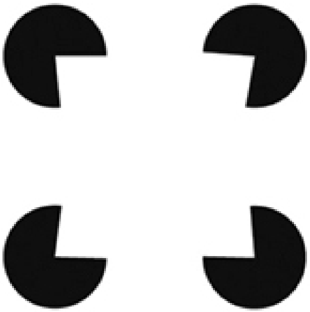

- Human tend to "see" invisible boundaries that yield plausible objects.
- Important mechanism of the human visual system to interpret the 3D world under normal conditions.
- Provides strong clues for depth recognition [Nitzberg, Mumford, Shiota '93].
- Psychophysical experiments suggest that those boundaries are well modeled by **elastic curves** [Kanizsa '79].

Subjective boundaries

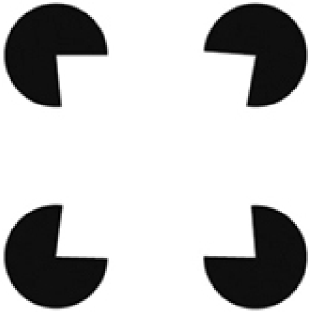

- Human tend to “see” invisible boundaries that yield plausible objects.
- Important mechanism of the human visual system to interpret the 3D world under normal conditions.
- Provides strong clues for depth recognition [Nitzberg, Mumford, Shiota '93].
- Psychophysical experiments suggest that those boundaries are well modeled by **elastic curves** [Kanizsa '79].

The Elastica functional

- ...obtained from minimizers of the Elastica energy

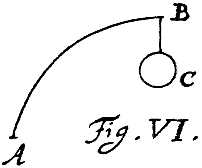

$$\int_\Gamma (1 + \alpha^2 |\kappa|^2) \, d\gamma \, , \; \alpha > 0.$$

- Long history, dating back at least to Bernoulli (1691) and Euler (1744)

Generalization to images

The Elastic curve energy can be generalized to whole images by imposing the Elastica energy to each level line of an image $u \in \mathcal{C}_c^2(\Omega, \mathbb{R})$ [Masnou, Morel '98], [Ambrosio, Masnou '03]

$$\int_\Omega \left(1 + \alpha^2 \left|\operatorname{div} \frac{\nabla u}{|\nabla u|}\right|^2\right) \, \mathrm{d}|\nabla u| \, ,$$

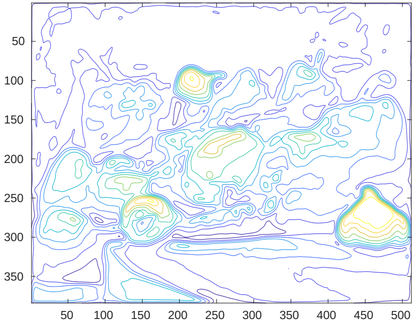

Minimizing the Elastica energy

- The Elastica energy is highly non-convex and hence is difficult to minimize directly
- Involves higher-order derivatives and hence is difficult to discretize and minimize [Chan, Kang, Shen '03].
- Recent approaches are based on Augmented Lagrangian approaches, which amounts to solving a non-convex saddle-point problem [Tai, Hahn, Chung '11], [Yashtini, Kang '15], [Bae, Tai, Zhu '17], [Dweng, Glowinsky, Tai '18].
- Related methods exist in the PDE community, e.g. Weickert's EED [Weickert '96] or joint interpolation of vector fields and intensities [Ballester, Bertalmio, Caselles, Sapiro, Verdera '03]
- In shape processing, phase-field methods have successfully been used to minimize the Willmore energy [Franken, Rumpf, Wirth '10], [Dondl, Mugnai, Röger '13], [Bretin, Masnou, Oudet '13]

Visual cortex

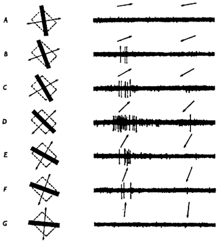

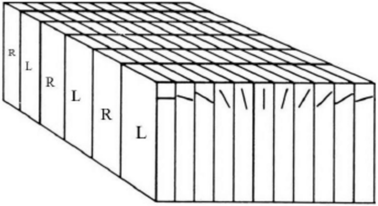

- Experiments suggest that the visual cortex is made of orientation sensitive layers [Hubel, Wiesel '59]
- Cells are connected between the layers to get a sense of curvature at objects boundaries

Mathematical models of the visual cortex

- The basic idea for a mathematical model is to keep the local orientation of the boundary as a separate variable.
- Related to the "Gauss map" $(x, \nu(x))$ [Anzelotti '88] and also "curvature varifolds" [Hutchinson '86].
- In image processing, the idea is to represent image boundaries (gradients) in the Roto-translation (RT) space $\Omega \times \mathbb{S}^1$.
- Use the sub-Riemannian structure of the RT space to describe the geometry of the visual cortex [Koenderink, van Doorn '87], [Hoffman '89], [Zucker '00], [Petitot, Tondut '98/'03], [Citti, Sarti '03/'06].
- Sub-Riemannian diffusion in the RT space for inpainting and denoising problems [Citti, Sarti '03/'06], [Franken, Duits '10], [Boscain, Chertovskih, Gauthier, Remizov '14], [Citti, Franceschiello, Sanguinetti, Sarti '15], [Duits et al. '19]
- Geodesics (minimal paths) by solving an anisotropic Eikonal equation [Mirebeau '14, '17], [Duits et al. '14, '16], [Mirebeau '18]

Variational / energy minimization approaches

- LP relaxations / discrete optimization on graphs [Schoenemann, Cremers '07], [Schoenemann, Kahl, Cremers '09], [El Zehiry, Grady '10], [Strandmark, Kahl '11], [Nieuwenhuis, Toeppe, Gorelick, Veksler, Boykov '14]
- Total vertex regularization (TVX) [Bredies, P. Wirth '13], uses curvature penalizations in the 3D RT $\Omega \times \mathbb{S}^1$ space based on a metric on $\mathbb{S}^1$ (not quadartic curvature).
- Extension of the lifting idea to a 4D space $\Omega \times \mathbb{S}^1 \times \mathbb{R}$ [Bredies, P. Wirth '15] to penalize the quadratic curvature.

Variational / energy minimization approaches

- LP relaxations / discrete optimization on graphs [Schoenemann, Cremers '07], [Schoenemann, Kahl, Cremers '09], [El Zehiry, Grady '10], [Strandmark, Kahl '11], [Nieuwenhuis, Toeppe, Gorelick, Veksler, Boykov '14]
- Total vertex regularization (TVX) [Bredies, P. Wirth '13], uses curvature penalizations in the 3D RT $\Omega \times \mathbb{S}^1$ space based on a metric on $\mathbb{S}^1$ (not quadartic curvature).
- Extension of the lifting idea to a 4D space $\Omega \times \mathbb{S}^1 \times \mathbb{R}$ [Bredies, P. Wirth '15] to penalize the quadratic curvature.

- This talk: arbitrary convex function (also quadratic) of the curvature in the 3D RT space $\Omega \times \mathbb{S}^1$.

Parametrized curves in the plane

- Consider the boundary of a smooth 2D set $E \subset \Omega \subseteq \mathbb{R}^2$ represented by a parametrized curve $\gamma(t) = (x_1(t), x_2(t))$ with parameter $t \in [0, 1]$.

Parametrized curves in the plane

- Consider the boundary of a smooth 2D set $E \subset \Omega \subseteq \mathbb{R}^2$ represented by a parametrized curve $\gamma(t) = (x_1(t), x_2(t))$ with parameter $t \in [0, 1]$.
- Its arc length variation is given by

$$\frac{\mathrm{d}s}{\mathrm{d}t} = |\dot{\gamma}(t)| = \sqrt{(\dot{x}_1(t))^2 + (\dot{x}_2(t))^2}$$

Parametrized curves in the plane

- Consider the boundary of a smooth 2D set $E \subset \Omega \subseteq \mathbb{R}^2$ represented by a parametrized curve $\gamma(t) = (x_1(t), x_2(t))$ with parameter $t \in [0, 1]$.
- Its arc length variation is given by

$$\frac{\mathrm{d}s}{\mathrm{d}t} = |\dot{\gamma}(t)| = \sqrt{(\dot{x}_1(t))^2 + (\dot{x}_2(t))^2}$$

- The tangential angle $\theta(t)$ is such that

$$\frac{\dot{\gamma}(t)}{|\dot{\gamma}(t)|} = (\cos\theta(t), \sin\theta(t))$$

Parametrized curves in the plane

- Consider the boundary of a smooth 2D set $E \subset \Omega \subseteq \mathbb{R}^2$ represented by a parametrized curve $\gamma(t) = (x_1(t), x_2(t))$ with parameter $t \in [0, 1]$.
- Its arc length variation is given by

$$\frac{\mathrm{d}s}{\mathrm{d}t} = |\dot{\gamma}(t)| = \sqrt{(\dot{x}_1(t))^2 + (\dot{x}_2(t))^2}$$

- The tangential angle $\theta(t)$ is such that

$$\frac{\dot{\gamma}(t)}{|\dot{\gamma}(t)|} = (\cos\theta(t), \sin\theta(t))$$

- The curvature κ_E of ∂E is defined as the ratio between the variation of the tangential angle θ and the variation of its length s, that is

$$\kappa_E = \frac{d\theta}{\mathrm{d}s} = \frac{\frac{\mathrm{d}\theta}{\mathrm{d}t}}{\frac{\mathrm{d}s}{\mathrm{d}t}} = \frac{\frac{\mathrm{d}\theta}{\mathrm{d}t}}{\sqrt{(\dot{x}_1(t))^2 + (\dot{x}_2(t))^2}}$$

Lifting the curve

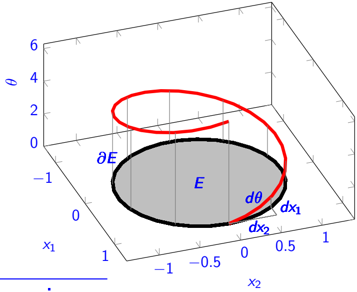

- We now "lift" the 2D curve $\gamma(t)$ to a 3D curve $\Gamma(t) = (x_1(t), x_2(t), \theta(t))$ in the RT space $\Omega \times \mathbb{S}^1$:
- The length of the lifted curve is given by

$$\begin{aligned}
\int_0^1 |\dot{\Gamma}(t)| \, \mathrm{d}t &= \int_0^1 \sqrt{(\dot{x}_1(t))^2 + (\dot{x}_2(t))^2 + (\dot{\theta}(t))^2} \, \mathrm{d}t \\
&= \int_0^1 \sqrt{1 + \frac{(\dot{\theta}(t))^2}{(\dot{x}_1(t))^2 + (\dot{x}_2(t))^2}} \sqrt{(\dot{x}_1(t))^2 + (\dot{x}_2(t))^2} \, \mathrm{d}t \\
&= \int_0^L \sqrt{1 + \kappa_E^2} \, \mathrm{d}s
\end{aligned}$$

- Length of the curve in the lifted space has a "sense" of curvature!
- How can we generalize this to more general energies involving the curvature?

Normalized tangential field

- We define the tangential vector $p(t) = (p^x(t), p^\theta(t))$ where

$$p^x(t) = (\dot{x}_1(t), \dot{x}_2(t)), \quad p^\theta(t) = \dot{\theta}(t), \quad |p^x(t)| = \sqrt{(\dot{x}_1(t))^2 + (\dot{x}_2(t))^2}$$

- We further define the normalized tangential field $\tau(x,\theta) = (\tau^x(x,\theta), \tau^\theta(x,\theta))$ in $\Omega \times \mathbb{S}^1$

$$\tau(x(t), \theta(t)) = \frac{p(t)}{|p(t)|}, \ \forall t \in [0,1]$$

- The curvature is therefore given by

$$\kappa_E(t) = \frac{p^\theta(t)}{|p^x(t)|} = \frac{\tau^\theta(x(t),\theta(t))}{|\tau^x(x(t),\theta(t))|},$$

Curvature penalizing energies

- We consider $f : \mathbb{R} \to [0, +\infty]$ a convex, lower-semicontinuous function and want to define a lower-semicontinuous extension to energies of the type

$$E \mapsto \int_{\partial E} f(\kappa_E) \, \mathrm{d}\mathcal{H}^1,$$

  where $E \subset \Omega$ is a set with C^2 boundary, and κ_E is the curvature of the set.
- Using the normalized tangential vector field $\tau(x, \theta)$, the energy can be extended to $\Omega \times \mathbb{S}^1$:

$$\int_{\partial E} f(\kappa_E) \, \mathrm{d}\mathcal{H}^1 = \int_{\Omega \times \mathbb{S}^1} f(\tau^\theta / |\tau^x|) |\tau^x| \, \mathrm{d}\mathcal{H}^1 \llcorner \Gamma_E,$$

  where Γ_E is the lifted curve.
- Note that the expression $f(\tau^\theta / |\tau^x|) |\tau^x|$ is in the form of the perspective of a convex function.

Different convex energies

$$\int_{\Omega\times\mathbb{S}^1} f(\tau^\theta/|\tau^x|)|\tau^x| \,\mathrm{d}\mathcal{H}^1 \llcorner \Gamma_E$$

[1] Also known as Reeds-Shepp model for cars [Reeds, Shepp '90]

Different convex energies

$$\int_{\Omega \times \mathbb{S}^1} f(\tau^\theta / |\tau^x|)|\tau^x| \,\mathrm{d}\mathcal{H}^1 \llcorner \Gamma_E$$

- $f_1(s) = 1 + \alpha|s|$: Total Absolute Curvature

$$\int_{\Omega \times \mathbb{S}^1} |\tau^x| + \alpha|\tau^\theta| \,\mathrm{d}\mathcal{H}^1 \llcorner \Gamma_E.$$

[1] Also known as Reeds-Shepp model for cars [Reeds, Shepp '90]

Different convex energies

$$\int_{\Omega \times \mathbb{S}^1} f(\tau^\theta / |\tau^x|)|\tau^x| \, \mathrm{d}\mathcal{H}^1 \llcorner \Gamma_E$$

- $f_1(s) = 1 + \alpha|s|$: Total Absolute Curvature

$$\int_{\Omega \times \mathbb{S}^1} |\tau^x| + \alpha|\tau^\theta| \, \mathrm{d}\mathcal{H}^1 \llcorner \Gamma_E.$$

- $f_2(s) = \sqrt{1 + \alpha^2 |s|^2}$: Total Roto-Translational Variation [1]

$$\int_{\Omega \times \mathbb{S}^1} \sqrt{|\tau^x|^2 + \alpha^2|\tau^\theta|^2} \, \mathrm{d}\mathcal{H}^1 \llcorner \Gamma_E$$

[1] Also known as Reeds-Shepp model for cars [Reeds, Shepp '90]

Different convex energies

$$\int_{\Omega\times\mathbb{S}^1} f(\tau^\theta/|\tau^x|)|\tau^x| \, \mathrm{d}\mathcal{H}^1 \llcorner \Gamma_E$$

- $f_1(s) = 1+\alpha|s|$: Total Absolute Curvature

$$\int_{\Omega\times\mathbb{S}^1} |\tau^x| + \alpha|\tau^\theta| \, \mathrm{d}\mathcal{H}^1 \llcorner \Gamma_E.$$

- $f_2(s) = \sqrt{1+\alpha^2|s|^2}$: Total Roto-Translational Variation [1]

$$\int_{\Omega\times\mathbb{S}^1} \sqrt{|\tau^x|^2 + \alpha^2|\tau^\theta|^2} \, \mathrm{d}\mathcal{H}^1 \llcorner \Gamma_E$$

- $f_3(s) = 1+\alpha^2|s|^2$: Total Squared Curvature

$$\int_{\Omega\times\mathbb{S}^1} |\tau^x| + \alpha^2\frac{|\tau^\theta|^2}{|\tau^x|} \, \mathrm{d}\mathcal{H}^1 \llcorner \Gamma_E.$$

[1] Also known as Reeds-Shepp model for cars [Reeds, Shepp '90]

Different convex energies

$$\int_{\Omega\times\mathbb{S}^1} f(\tau^\theta/|\tau^x|)|\tau^x| \,\mathrm{d}\mathcal{H}^1 \llcorner \Gamma_E$$

- $f_1(s) = 1 + \alpha|s|$: Total Absolute Curvature

$$\int_{\Omega\times\mathbb{S}^1} |\tau^x| + \alpha|\tau^\theta| \,\mathrm{d}\mathcal{H}^1 \llcorner \Gamma_E.$$

- $f_2(s) = \sqrt{1+\alpha^2|s|^2}$: Total Roto-Translational Variation [1]

$$\int_{\Omega\times\mathbb{S}^1} \sqrt{|\tau^x|^2 + \alpha^2|\tau^\theta|^2} \,\mathrm{d}\mathcal{H}^1 \llcorner \Gamma_E$$

- $f_3(s) = 1 + \alpha^2|s|^2$: Total Squared Curvature

$$\int_{\Omega\times\mathbb{S}^1} |\tau^x| + \alpha^2 \frac{|\tau^\theta|^2}{|\tau^x|} \,\mathrm{d}\mathcal{H}^1 \llcorner \Gamma_E.$$

$\boxed{\text{Convex energies in the measure } \sigma = \tau \,\mathrm{d}\mathcal{H}^1 \llcorner \Gamma_E}$

[1] Also known as Reeds-Shepp model for cars [Reeds, Shepp '90]

The measure σ

The measure $\sigma = \tau \, \mathrm{d}\mathcal{H}^1 \llcorner \Gamma_E$ is not arbitrary: It satisfies two important constraints:

(i) By construction, it is a circulation and has zero divergence in $\Omega \times \mathbb{S}^1$ since we want to represent closed curves (or ending at the boundary).

(ii) Its marginals in $\Omega \times \mathbb{S}^1$, denoted by $\bar{\sigma} = \int_{\mathbb{S}^1} \sigma^x$ also have zero divergence.

(iii) It follows that there exists a BV function u such that $Du^\perp = \bar{\sigma}$, here u is the characteristic function of the set E.

Convex representation

- We define the following convex function

$$h(\theta, p) = \begin{cases} |p^x| f(p^\theta/|p^x|) & \text{if } p^x \in \mathbb{R}_+\theta, p^x \neq 0, \\ f^\infty(p^\theta) & \text{if } p^x = 0, \\ +\infty & \text{else.} \end{cases},$$

where $f^\infty(t) = \lim_{s\to 0} sf(t/s)$ is the recession function of f.

- This function encodes the sub-Riemannian structure of $\Omega \times \mathbb{S}^1$.
- It is well known that h is a one-homogeneous function, hence the support function of a convex set, that is

$$h(\theta, p) = \sup_{\xi \in H(\theta)} \xi \cdot p$$

where the convex set $H(\theta)$ is given by:

$$H(\theta) = \{\xi = (\xi^x, \xi^\theta) \in \mathbb{R}^3 : \xi^x \cdot \underline{\theta} \leq -f^*(\xi^\theta)\}, \quad \underline{\theta} = (\cos\theta, \sin\theta)$$

Visualization of the set $H(\theta)$

Example using $f(t) = 1 + \alpha^2 t^2$ (Elastica):

$$H(\theta) = \{\xi = (\xi^x, \xi^\theta) \in \mathbb{R}^3 : \xi^x \cdot \underline{\theta} + \frac{(\xi^\theta)^2}{(2\alpha)^2} \leq 1\}$$

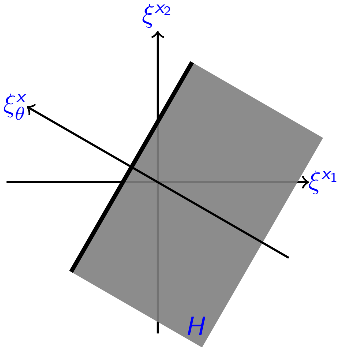

(a) $H \cap \{(\xi^x, \xi^\theta) : \xi^x \in \mathbb{R}^2, \xi^\theta = 0\}$

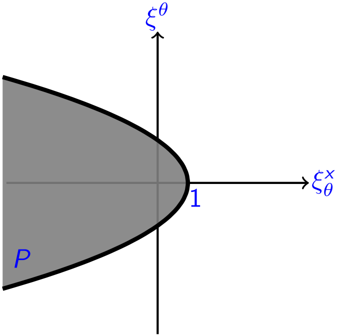

(b) Profile P

The functional

- We introduce the following functional:

$$\boxed{F(u) = \inf \left\{ \int_{\Omega \times \mathbb{S}^1} h(\theta, \sigma) \; : \; \operatorname{div} \sigma = 0, \; \bar{\sigma} = Du^{\perp} \right\}}$$

- In general, σ is a bounded Radon measure, therefore the correct way to write the energy is rather

$$\int_{\Omega \times \mathbb{S}^1} h\left(\theta, \frac{\sigma}{|\sigma|}\right) d|\sigma|.$$

  and the constraints are understood in the weak sense.
- We assume that $f(t) \geq \gamma\sqrt{1+t^2}$ such that

$$F(u) \geq \gamma \int_{\Omega \times \mathbb{S}^1} |\sigma| \geq \gamma \int_{\Omega} |Du|$$

- It can be shown that the functional is convex, lower-semicontinuous on $BV(\Omega)$, since

$$\int_{\Omega \times \mathbb{S}^1} h(\theta, \sigma) = \sup_{\varphi(x,\theta) \in H(\theta)} \int_{\Omega \times \mathbb{S}^1} \varphi \cdot \sigma$$

Tightness of the representation

We can show the following result:

Theorem

Let $E \subset \Omega$ be a set with C^2 boundary. Then

$$F(\chi_E) = \int_{\partial E \cap \Omega} f(\kappa_E(x)) d\mathcal{H}^1(x).$$

- The proof is based on Smirnov's theorem (1994), which shows that if σ is a measure with $\operatorname{div} \sigma = 0$ then it is a superposition of curves.
- We conjecture that our result can be extended to general BV functions u with C^2 level sets, hence coinciding with Masnou and Morel's model.
- We could hope that $F(u)$ is the lower-semicontinuous envelope of the original functional, however, simple examples show that this is not the case [Bellettini, Mugnai '04/'05], [Dayrens, Masnou '16].

Dual representation

- Recall our primal functional

$$F(u) = \inf \left\{ \int_{\Omega\times\mathbb{S}^1} h(\theta,\sigma) \,:\, \operatorname{div}\sigma = 0,\ \bar{\sigma} Du^{\perp} \right\}.$$

- It has the following dual representation

$$\begin{aligned} F(u) \quad = \quad & \sup \left\{ \int_{\Omega} \psi \cdot Du^{\perp} \,:\, \psi \in C_c^0(\Omega;\mathbb{R}^2), \right. \\ & \left. \exists\, \varphi \in C_c^1(\Omega\times\mathbb{S}^1), \underline{\theta}\cdot(\nabla_x\varphi + \psi) + f^*(\partial_\theta\varphi) \le 0 \right\}. \end{aligned}$$

- Coincides with the dual representation in our previous work [Bredies, P. Wirth '15] which is based on an explicit lifting of the curvature variable.
- In our approach the curvature variable appears naturally as the derivative of the orientation.

Discretization

- We use a staggered 2D-3D averaged Raviart-Thomas finite elements discretization based on cubes.
- Divergence-conforming discretization, uses a cube-center-based quadrature rule for the energy.
- We can show consistency of the discretization up to small oscillations.

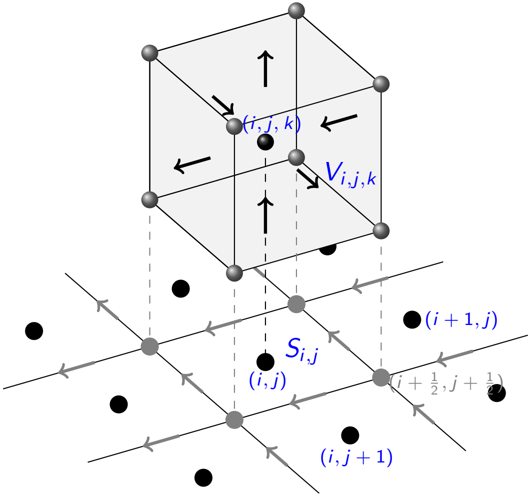

Discrete Problem

- The consider discrete optimization problems of the form

$$\min_u F_\delta(u) + G_\delta(u),$$

with

$$F_\delta(u) = \min_\sigma \left\{ \delta_x^2 \delta_\theta \sum_{\mathbf{j}=(i,j,k)\in\mathcal{J}} h(k\delta_\theta, (\mathcal{A}\sigma)_\mathbf{j}) : \mathcal{D}\sigma = 0,\ \mathcal{P}\sigma - \mathcal{G}u = 0 \right\}.$$

- We solve this non-smooth convex optimization problem by considering its Lagrangian

$$\begin{aligned}\min_{u,\sigma} \max_{\phi,\psi,\xi} \quad & \sum_{\mathbf{j}\in\mathcal{J}} (\mathcal{A}\sigma)_\mathbf{j} \cdot \xi_\mathbf{j} - \sum_{\mathbf{j}=(i,j,k)\in\mathcal{J}} h^*(k\delta_\theta, \xi_\mathbf{j}) + G_\delta(u) + \\ & \sum_{\mathbf{j}\in\mathcal{J}} (\mathcal{D}\sigma)_\mathbf{j} \phi_\mathbf{j} + \sum_{\mathbf{i}\in\mathcal{I}^1\cup\mathcal{I}^2} ((\mathcal{P}\sigma)_\mathbf{i} - (\mathcal{G}u)_\mathbf{i})\, \psi_\mathbf{i},\end{aligned}$$

- We solve the saddle-point problem with a pre-conditioned first-order primal-dual algorithm.

First experiment: computing a disk

- Consider the Elastica energy for the boundary of a disk

$$\int_{\partial B(0,r)} (1+\alpha^2\kappa^2)\, d\mathcal{H}^1 = 2\pi(r+\alpha^2/r)$$

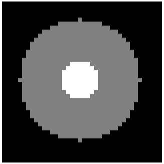

- The energy is minimized for $r = 1/\alpha$.
- We study the effect of different discretizations of the angular dimension by computing (via inpainting) a disk of radius $r = 10$.

N_θ	H_{TV} $(2\pi r \approx 62.83)$	H_{AC} $(2\pi \approx 6.28)$	H_{SC} $(2\pi/r \approx 0.62)$
4	60.10	6.34	1.75
8	54.80	6.28	0.89
16	58.50	6.28	0.70
32	61.52	6.28	0.64
64	62.93	6.28	0.62

Disk inpainting

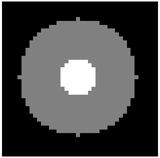

(a) u^0

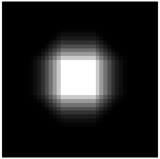

(b) $N_\theta = 4$

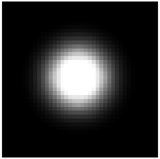

(c) $N_\theta = 8$

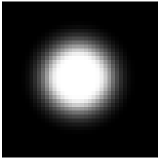

(d) $N_\theta = 16$

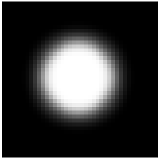

(e) $N_\theta = 32$

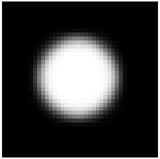

(f) $N_\theta = 64$

Visualization of the measure σ

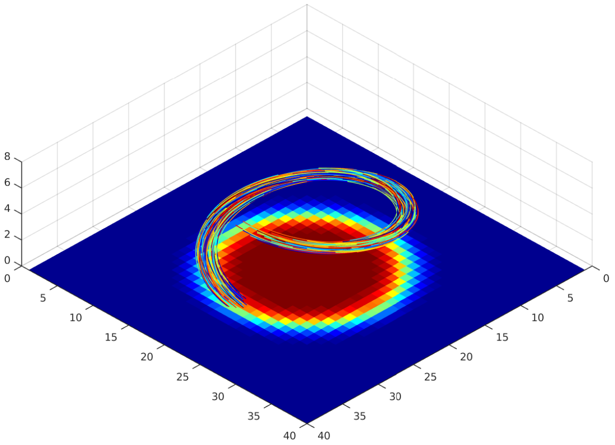

Where it fails: Non-smooth level sets

- We consider the following inpainting problem by minimizing the Elastica energy.

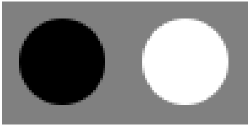

(a) Original image

(b) Input image u^0

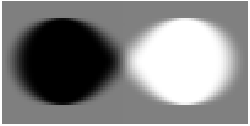

(c) Computed image u

- The energy of the original Elastica energy should be infinite
- Our convexification finds a lower energy solutions with non-smooth level sets

Visualization of the measure σ

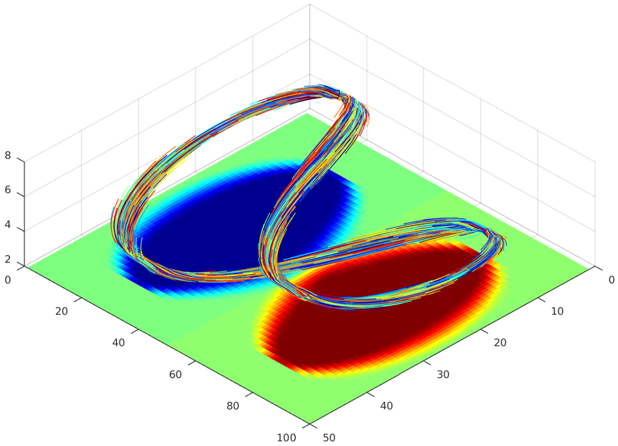

Shape regularization

- We consider the problem of regularizing a given shape

Shape regularization

(a) TAC, $\lambda = 8$

(b) TAC, $\lambda = 4$

(c) TAC, $\lambda = 2$

Shape regularization

(a) TRV, $\lambda = 8$ (b) TRV, $\lambda = 4$ (c) TRV, $\lambda = 2$

Shape regularization

(a) TSC, $\lambda = 8$

(b) TSC, $\lambda = 4$

(c) TSC, $\lambda = 2$

Shape completion (1)

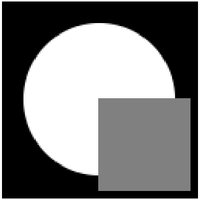

(a) Input image

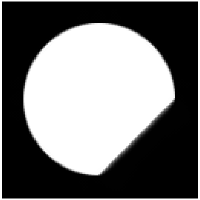

(b) TAC, $\alpha = 15$

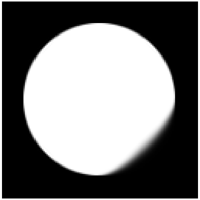

(c) TRV, $\alpha = 15$

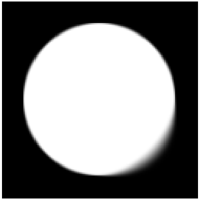

(d) TSC, $\alpha = 50$

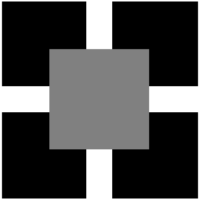

(e) Input image

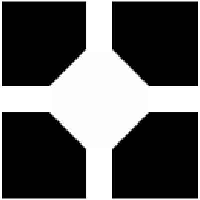

(f) TAC, $\alpha = 15$

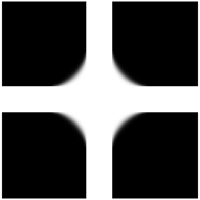

(g) TRV, $\alpha = 15$

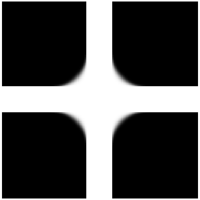

(h) TSC, $\alpha = 10$

Shape completion (2)

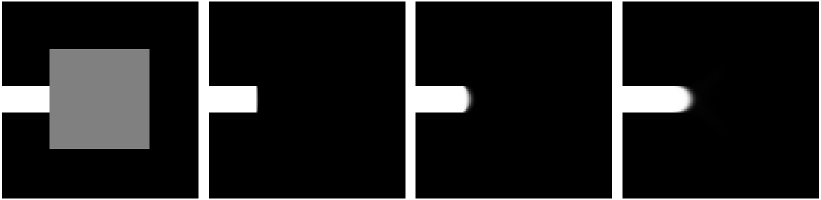

(a) Input image (b) TAC, $\alpha = 15$ (c) TRV, $\alpha = 15$ (d) TSC, $\alpha = 10$

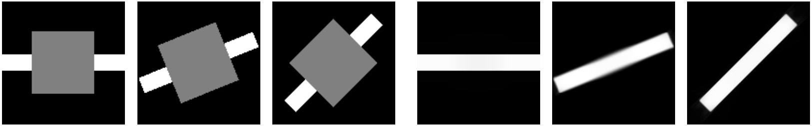

(e) Input images with rotations $0, \pi/8, \pi/4$ (f) TAC, $\alpha = 15$

Weickert's cat

- Shape reconstruction from "dipole" data
- The dipoles are original data from J. Weickert.

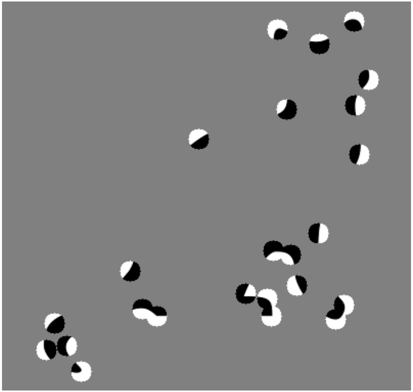

Dipole data

Weickert's cat

- Shape reconstruction from “dipole” data
- The dipoles are original data from J. Weickert.

Minimizing the TSC energy

Weickert's cat

- Shape reconstruction from "dipole" data
- The dipoles are original data from J. Weickert.

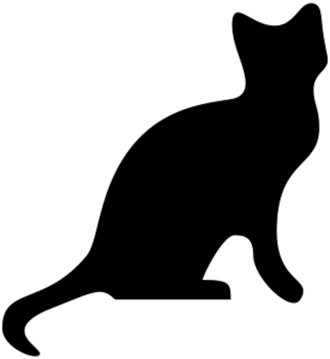

Original shape

Image inpainting

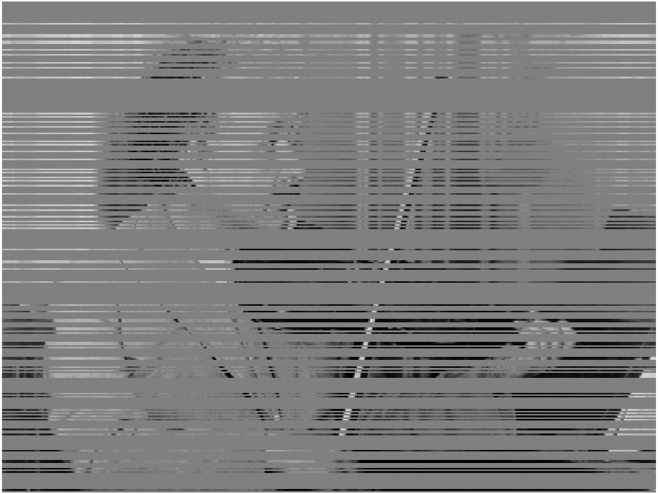

Input

Image inpainting

TV

Image inpainting

TSC

Image inpainting

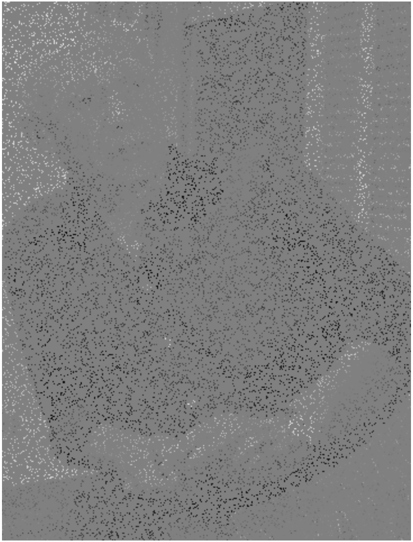

Input

Image inpainting

TV

Image inpainting

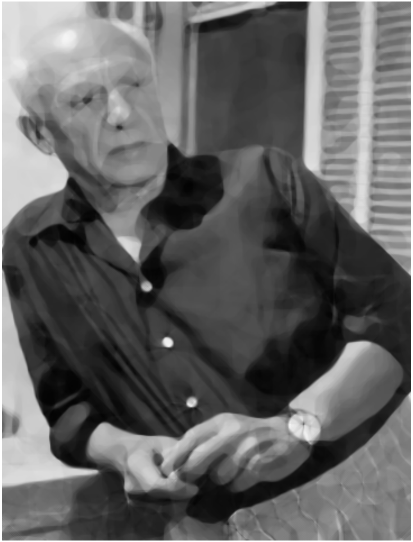

TSC

Image denosing: Guassian noise

Input

Image denosing: Guassian noise

TV, $\alpha = 0$, $\lambda = 10$

Image denosing: Guassian noise

TSC, $\alpha = 10$, $\lambda = 40$

Image denosing: S & P noise

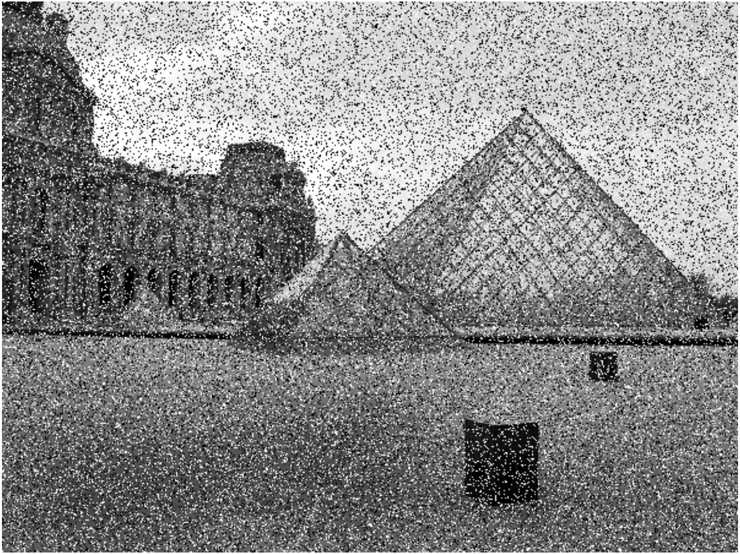

Input

Image denosing: S & P noise

TV, $\alpha = 0$, $\lambda = 2$

Image denosing: S & P noise

TSC, $\alpha = 10$, $\lambda = 7$

Conclusion

- **Convex representation of curvature penalizing variational models for shape and image processing**
- Tightness result for C^2 shapes
- Functional is below the convex envelope of the original energy
- Discretization based on staggered averaged Raviart-Thomas finite elements
- Numerical computation using primal-dual schemes
- A fine resolution of the angular domain is necessary to faithfully approximate squared curvature
- Application to various shape and image processing problems

Conclusion

- **Convex representation of curvature penalizing variational models for shape and image processing**
- Tightness result for C^2 shapes
- Functional is below the convex envelope of the original energy
- Discretization based on staggered averaged Raviart-Thomas finite elements
- Numerical computation using primal-dual schemes
- A fine resolution of the angular domain is necessary to faithfully approximate squared curvature
- Application to various shape and image processing problems

Thank you for listening!

European Research Council
Established by the European Commission

Der Wissenschaftsfonds.